Analysis of Load Carrying Capability of A Morphing Composite Wing Structure

ANJU ANIL
Dept.of Aeronautical Engineering,
Excel Engineering College
anjuanildilna@gmail.com

SINCY CHACKO, M.E.,
 Asst. Professor
 Dept. of Aeronautical Engineering
 ILMCET, Perumbavoor
 sincyc134@gmail.com

D.VADIVEL, M.E.,
Asst. Professor
Dept.of Aeronautical Engineering
Excel Engineering College

Abstract: One of the main challenges for the civil aviation industry is the reduction of its environmental impact. Over the past years, improvements in performance efficiency have been achieved by simplifying the design of the structural components and using composite materials to reduce the overall weight. The parameters of the key structural components, such as skin, spars, ribs and stringers were set to satisfy the static stress and buckling requirements. Moreover, numerical and experimental studies were conducted to analyze the static failure and buckling behavior of two typical composite wing structural components: a spar section and a web and base joint assembly. The aerodynamic distributed load on the wing creates shear force, bending moment and tensional moment at wing stations. Static load carrying capability of the wing box is carried out through a linear static stress analysis. The top skin of the wing box will experience the axial compression during wing bending. Significant changes in drag reduction and fuel consumption can be obtained by using smart morphing structures. This will significantly improve the aircraft efficiency.

Keywords: Morphing.

INTRODUCTION

The current goal for the civil aviation industry is to improve the efficiency and performance of the aircraft in order to reduce the impact on the environment and also to minimize the costs incurred by the airlines without compromising all the safety aspects. The state of the art wing design is characterized by a central wing box which provides stiffness and strength to the structure in order to be able to withstand the high aerodynamic loads, and also holds most of the fuel carried by the aircraft. Replacing this rigid structure with a morphing one would cause many complications as the required rigidity would be lost, and it would be necessary to create an alternative storage for the fuel. On the other hand, if morphing structures are used to replace only the movable high lift devices, a more laminar flow can be obtained without compromising the conventional wing box concept. Smart morphing high lift devices will also offer many more advantages in addition to flow laminarisation. Furthermore, versatile high lift devices can be used to reduce off-design effect. This feature is of special relevance to laminar wings where off-design effect cause severe problems with the transonic shock. The design for the next generation wing proposed by this project uses an innovative concept to achieve a smart leading edge, to achieve a smooth seamless surface for flow laminarisation and noise reduction, and composite materials to maximize the stiffness to weight ratio. The main research objectives can be summarized as follows:

 To carry out a structural analysis of a composite wing box and its interface with the control surface, investigating in particular on the mechanical behavior of composite structural components and exploring new methods to increase their structural efficiency and load carrying capability. To develop an innovative design concept for the actuation mechanism for the morphing leading edge device of a large commercial aircraft wing.

 To conduct a static and dynamic analysis of the morphing leading edge structure and fully demonstrate its design and structural feasibility.

In order to achieve these objectives numerical and experimental studies were conducted to analyze the static failure and buckling behavior of two typical composite wing structural components: a spar section and a web and base joint assembly. A design for the morphing leading edge actuation mechanism was developed and a geometrical non-linear finite element analysis was conducted to simulate the leading edge morphing deflection and ensure that the skins satisfied the structural strength requirements. To prove that the proposed actuation system can compete with the conventional rigid rib, the behavior of the skin integrated with the internal actuation mechanism was tested under the aerodynamic pressure and gust loads.

Several morphing wing concepts have been developed in the past however, they are mostly applied to micro air vehicles or small unmanned vehicles, and concepts for smart high lift devices for larger commercial aircraft are not readily available. Some of these designs can be taken as a starting point for the development of smart high lift devices, in particular they are mostly suitable to be used for an adaptive flap, however before a feasible morphing wing can be designed, further study and improvements are required. This sets the scene for the research on smart high lift devices for next generation wing.

II. COMPOSITE STRUCTURES THEORETICAL BACKGROUND AND ANALYSIS TOOLS

Composite materials are made of continuous or discontinuous fibers embedded in a matrix. The directional nature of these fibers in the ply, introduces a directional dependence to the composite layer properties. These materials are classified as orthotropic. The mechanical behavior of composite materials differs from that of isotropic materials, since two directions must be considered for the strength and stiffness properties.

STRUCTURAL ANALYSIS OF COMPOSITE AIRCRAFT COMPONENTS

A particular characteristic of composite materials is that stiffness and strength properties depend on the direction of the fibers in the laminates. The behavior of these materials, when loaded, is therefore different from isotropic materials and many more parameters must be considered to predict them.

STIFFNESS OF ORTHOTROPIC LAMINATES USING THE CLASSICAL LAMINATION THEORY

For unidirectional fiber reinforced lamina, there are two perpendicular planes of symmetry that define the principal axes of the material properties. These principal axes correspond to the direction of the fibers and a direction transverse to the fibers, and are denoted by the subscripts 1 and 2 respectively. This coordinate system is a local system associated with the single lamina. A global coordinate system, attached to a fixed reference point, is instead used when the whole laminate is considered.
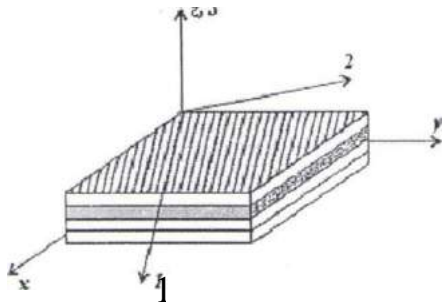

Fig. 1 Global and local coordinate system.

The stress-strain relationship in the global coordinate system is expressed as:

$$\begin{Bmatrix} \sigma_x \\ \sigma_y \\ \tau_{xy} \end{Bmatrix} = T^{-1}QRTR^{-1} \begin{Bmatrix} \varepsilon_x \\ \varepsilon_y \\ \gamma_{xy} \end{Bmatrix} = \begin{bmatrix} \overline{Q}_{11} & \overline{Q}_{12} & \overline{Q}_{16} \\ \overline{Q}_{12} & \overline{Q}_{22} & \overline{Q}_{26} \\ \overline{Q}_{16} & \overline{Q}_{21} & \overline{Q}_{66} \end{bmatrix} \begin{Bmatrix} \varepsilon_x \\ \varepsilon_y \\ \gamma_{xy} \end{Bmatrix}$$

σ_x – Direct Stress in X-axis
σ_y – Direct Stress in Y-axis
τ_{xy} – Direct Shear Stress in xy-axis
T- Transformation Matrix
R – Reuter Matrix
ε_x – Direct Strain in X-axis
ε_y – Direct Strain in Y-axis
ε_{xy} –Direct Shear Strain in xy-axis
Q – Reduced Stiffness

In a laminate with N orthotropic layers perfectly bonded together with an infinitely thin bonded line and continuous in-plane deformations across the bond line

The following constitutive relation for the laminate can be defined:

$$\begin{Bmatrix} N_x \\ N_y \\ N_{xy} \\ M_x \\ M_y \\ M_{xy} \end{Bmatrix} = \begin{bmatrix} \begin{bmatrix} A_{11} & A_{12} & A_{16} \\ A_{12} & A_{22} & A_{26} \\ A_{16} & A_{26} & A_{66} \end{bmatrix} & \begin{bmatrix} B_{11} & B_{12} & B_{16} \\ B_{12} & B_{22} & B_{26} \\ B_{16} & B_{26} & B_{66} \end{bmatrix} \\ \begin{bmatrix} B_{11} & B_{12} & B_{16} \\ B_{12} & B_{22} & B_{26} \\ B_{16} & B_{26} & B_{66} \end{bmatrix} & \begin{bmatrix} D_{11} & D_{12} & D_{16} \\ D_{12} & D_{22} & D_{26} \\ D_{16} & D_{26} & D_{66} \end{bmatrix} \end{bmatrix} \begin{Bmatrix} \varepsilon_x^0 \\ \varepsilon_y^0 \\ \gamma_{xy}^0 \\ \kappa_x \\ \kappa_y \\ \kappa_{xy} \end{Bmatrix}$$

Nx – Force along 1 direction
Ny – Force along 2 direction
Mx – Moment along 1 direction
My – Moment along 2 direction
εx0 – Mid Plane Strain in 1 direction
εy0 – Mid Plane Strain in 2 direction
vxy0 – Mid Plane Shear Strain

Q – Reduced Stiffness

Kx & Ky – Curvature of laminate in 1 direction and 2 direction.Where [A], [B] and [D] matrices are the laminate stiffness matrix and are defined in terms of ply stiffness as:

$$A_{ij} = \sum_{k=1}^{N} \left(\overline{Q}_{ij} \right)_{(k)} (z_k - z_{k-1})$$

$$B_{ij} = \frac{1}{2} \sum_{k=1}^{N} \left(\overline{Q}_{ij} \right)_{(k)} (z_k^2 - z_{k-1}^2)$$

$$D_{ij} = \frac{1}{3} \sum_{k=1}^{N} \left(\overline{Q}_{ij} \right)_{(k)} (z_k^3 - z_{k-1}^3)$$

Where, [A] – Laminate Membrane

[B] – Coupling Stiffness

[D]- Bending Stiffness

These three matrices therefore, determine the stiffness of a laminate in different directions and describe the response of a laminate to inplane forces and moments.

COMPOSITE THIN- WALLED STRUCTURAL ANALYSIS

An aircraft can be considered as an assembly of panels ranging from open to multi-cell closed sections subject to bending, shear, torsional and axial loads. Because the thickness of these panels is small compared to the cross sectional dimensions,

these structures are often treated as thin walled beams. A detailed analysis of open and closed isotropic thin- walled beams under various types of loading can be found in.

FINITE ELEMENT ANALYSIS

The continuous structures are artificially idealized into a number of elements inter connected at the nodes and the matrix method of analysis is applied to determine forces and displacements. Commercially available software has made this analysis method more accessible. This section presents the approached used by the finite element software packages NASTRAN to carry out non linear static, buckling and dynamic analysis.

NON LINEAR STATIC ANALYSIS USING NASTRAN

- The structure is only subject to small displacement when the load is applied.
- The stress and strain relationship in the materials is linear.
- The boundary conditions remain constant

If one of the conditions is not satisfied nonlinear effects must be introduced: which can be geometric, material or boundary condition nonlinearities.

LINEAR BUCKLING ANALYSIS USING NASTRAN

A buckling analysis is used to determine the load at which the structure becomes instable: when the structure continues to deflect without an increase in magnitude of loading. When carrying out a linear buckling analysis, in the finite element method the stiffness of a structure is determined as the sum of the linear stiffness matrix and differential stiffness matrix. The differential stiffness matrix, which is a function of the geometry, element type and applied loads, represents the linear approximation of reducing the linear stiffness matrix in the case of a compressive load, and increasing the linear stiffness matrix in the case of a tensile load.

The inverse power method is a tracking method as it attempts to extract the lowest eigen value and eigen vector in a desired range. The enhanced inverse power method is similar to the inverse power method except that is uses Sturum sequence logic to ensure that all modes are found within the specified eigen value range.

It is and efficient method and if an eigen value cannot be extracted within the specified range a diagnostic message is issued. This method is the most recommended method when carrying out linear buckling analysis using NASTRAN.

DYNAMIC ANALYSIS USING NASTRAN

In a dynamic analysis the loads are applied to the structure as a function of time and consequently, the induced responses are also time dependent. This time varying characteristic makes dynamic analysis more complicated than static analysis. Three types of dynamic analysis can be performed with NASTRAN:

- Real eigen value analysis: used to determine the undamped free vibration behavior of a structure. The results of an eigen value analysis indicate the frequency and shape at which the structure tends to vibrate.
- Linear frequency response analysis: an efficient method for finding the steady-state response to

sinusoidal excitation. In a frequency response analysis, the loading is a sine wave for which the frequency, amplitude and phase are specified.

III. COMPOSITE WING BOX AND LEADING EDGE PRELIMINARY DESIGN AND ANALYSIS

The main aim of this research study is to achieve a feasible design for a morphing leading edge to be used as a high lift device on a short range commercial aircraft. However, before setting the details of the actuation system it was of paramount importance to ensure that the main wing box structure was able to withstand the external loads
.

THE REFERENCE BASELINE WING
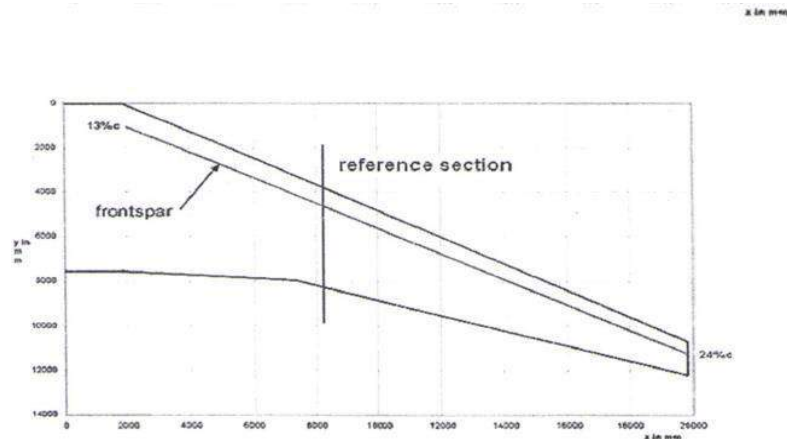
The reference baseline wing used in the current research was designed for a short range commercial aircraft and its general geometrical details were provided by one of the project partners.

Area(m2)	172
Aerodynamic mean chord(m)	5.15
Span(m)	39.65
Aspect Ratio	9.14
Taper Ratio	0.2
Root chord/percentage relative thickness(m)	16
Kink chord/percentage relative thickness(m)	11.5
Tip chord/percentage relative thickness(m)	10.5
Sweep angle outer wing (deg)	28

Table: Baseline Wing geometrical parameters

WING BOX SKIN PRELIMINARY DESIGN

This section presents how the wing box skin panel thickness and the stringers geometry were set at the wing reference section, where the wing box length was 1.855m, the front and rear spars were 0.438m and 0.364m in height respectively.
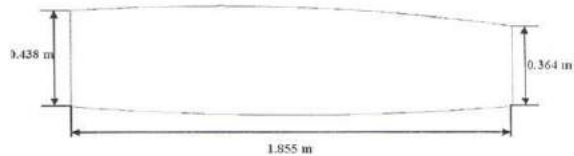
Figure: Wing box geometry at the reference section.

Two different thicknesses were used for the skin and stringers: 0.25mm and 0.184 respectively. The stringers ply were thinner in order to be able to obtain a suitable lay up for relatively thin laminates, while obeying the stacking sequence rules, and also to achieve finer changes in thickness to reduce the overall weight when carrying out optimization analysis scaling from the data available for an A320 wing, at the reference section, fourteen stringers were used to reinforce the wing box skin panels.

To maximize the effect of the stringers against buckling due to the aerodynamic loads I- shaped stringers were used on the upper wing cover. T- shaped stringers were instead used on the lower skin, since the risk of buckling was lower compared to the upper surface.

LEADING EDGE SKIN PRELIMINARY STRUCTURAL ANALYSIS

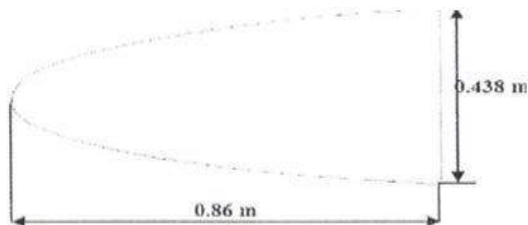The leading edge at the reference section was 0.86m in chord wise length and 0.44m in height.

Figure: Leading edge geometry at the wing reference section

The leading edge skin was reinforced by eight metallic I shaped stringers on both upper and lower skin panels and their flange and web were 12mm in length and 3mm in thickness. In the initial design two types of materials were selected for the leading edge skin: a metallic option, aluminium 2024-T81. The stress on the leading edge skin, due to the aerodynamic loading, was calculated using the same method as the one applied for the wing box skin, i.e, employing the TW box program. A double cell idealized model of the leading edge and wing box was created.

The wing box structure was included in this analysis in order to be able to apply the shear force through the aerodynamic center and the bending moment thought the elastic center.

IV.DESIGN AND ANALYSIS OF THE MORPHING LEADING EDGE

The study of the morphing leading edge structure was carried out at the wing reference section, where the wing chord

was 4m, when the leading edge structure was analyzed on its own a unit span section was considered, while when the wing box structure was also analyzed a 2m tapered section was considered.

THE WING BOX AND MORPHING LEADING EDGE GEOMETRY AND MATERIALS

The leading edge at the reference section was 0.86m chord wise, 1m span wise and 0.44m in height. The leading edge skin was reinforced by eight metallic I shaped stringers on both upper and lower skin panels, with 0.12m pitch distance, and their flange and web were 12mm in length and 3mm in thickness. In the initial design two types of materials were selected for the leading edge skin: a metallic option, aluminum 2024-T81 (Al), and glass fiber (GF). The aluminum skin was 2mm in thickness while the glass fiber skin was 3mm in thickness made of 12 layers arranged in a symmetrical layup [+45/03/90]s.

The wing box at the reference section was 1.855m, the front and rear spars were 0.438m and 0.364m in height respectively. The upper wing cover was reinforced by fourteen I shaped stringers (55mm*50mm*50mm) while the lower skin was reinforced by fourteen T- shaped stringers (50mm*50mm). Both skin and stringers were made of carbon fiber prepeg (HexTow IM7). However the skin laminate plies were 0.25mm thick while the stringers laminate plies were 0.184mm thick. The upper skin stringers web and flange laminates had the same layup as the skin but the total thickness was 13.616mm and the total mm. The stringers reinforcing the lower wing cover had the same layup as the skin but the flange and web thickness was 8.096mm.
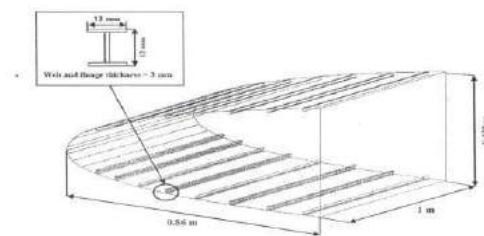
STRUCTURAL REQUIREMENTS

Several requirements were set for the leading edge structure and its morphing deflected shape in order to ensure a laminar flow over the wing. A smooth change in curvature was necessary in the deployed position therefore the upper and lower surfaces were gapless and 12% of the leading edge was considered to be rigid. Furthermore, to avoid strong suction peaks for high angles of attack, which lead to poor high lift behavior, the leading edge nose radius was required to increase, during deployment, to twice as large as the retracted position. The maximum vertical and horizontal displacements needed to obtain the required lift were 6% and 1.2% of the wing chord respectively.

THE AERODYNAMIC PRESSURE LOAD

The aerodynamic pressure over the wing section had a significant effect on the actuation load demand and stress distribution of the structure and it was therefore necessary to obtain accurate external loads. Results obtained from a computational fluid dynamics (CFD) simulation of a 2-D airfoil were used as pressure loads to be applied to the structure. According to the flight conditions three models were created. Mode 1 was for the clean configuration at cruise flight: cruise the aerodynamic pressure was calculated at 31000ft and the flow velocity was at Mach 0.8. In landing condition, the wing angle of attack was set at 12 degrees with flow velocity Mach 0.15 and a Reynolds number of 7*106. The atmospheric conditions were taken for an altitude of 20000ft and an air temperature of 248.6k.

MORPHING LEADING EDGE STATIC AEROELASTIC ANALYSIS

The eccentric beam actuation system is a feasible mechanism in terms of force and power demand. However, the leading edge skin material constraints were not yet considered. This type of study allowed to assess whether the skin material was appropriate to achieve the deflection without violating the mechanical strength limitations. This study was necessary to ensure that the eccentric beam actuation mechanism can provide adequate support to the skin when the structure was subject to the external loads.

NONLINEAR STATIC ANALYSIS OF THE WING BOX AND LEADING EDGE STRUCTURE

A nonlinear static analysis was conducted considering both the wing box and the leading edge so that the effect of the flexibility and elastic deformation of the high lift device on the main wing box structure could be evaluated. The study was carried out at all the three flight conditions: landing with the leading edge in neutral position, landing with the fully deployed leading edge and clean cruise configuration. In order to meet the safety requirements however, an ultimate load factor of 2.5g was applied to the wing box. This part of the structure was therefore subject to a pressure load 2.5 times larger than that of actual case. The wing section considered for this study case was tapered, 2m in span wise length and it was taken from the wing reference section outwards.

Due to its flexible nature, the leading edge skin was subject to relatively high elastic deformation: especially at landing when the pressure was greater towards the nose in order to produce higher lift. At cruise condition the leading edge skin elastic deflection was however much smaller. On the other hand the wing box was extremely stable compared to the leading edge structure and the maximum elastic deflection was 0.23mm in the landing configuration with the fully developed leading edge. The reduced stiffness of the high lift device did not have any effect on the behavior of the wing box.

Flight Condition	Beam deflection (mm)	Leading edge skin deflection (mm)	Wing box deflection(mm)
Landing with clean leading edge	6.83	12.1	0.1
Landing with deflected leading edge	11.9	15	0.023
Cruise clean configuration	2.17	2.33	0.05

## MORPHING LEADING EDGE DYNAMIC RESPONSE ANALYSIS

The final stage of the morphing leading edge study was to analyze its dynamic behavior. A modal analysis was firstly conducted to obtain the natural frequencies and mode shapes of the structure with the integrated actuation system. Then, a frequency and gust response analysis, at both landing and cruise conditions, were carried out. The effect of the actuator stiffness at the root of the eccentric beam was also taken into account by changing the beam stiffness at root as explained for the static case.

NATURAL VIBRATION ANALYSIS

The leading edge vibration analysis was carried out for both deployed and clean configurations. In landing configuration the first natural frequency was lower than that in cruise, and the corresponding mode was a disc vibration mode. The first beam mode at landing condition occurred at 73Hz when the root stiffness was 100% and 53Hz when the root stiffness was 10%. Furthermore, the first beam vibration mode at cruise condition for the 100% beam root stiffness was 64Hz: however this was reduced by 25% when the beam root stiffness was reduced to 10%. The skin first vibration mode occurred instead at the higher modes: 77Hz and 134Hz when the leading edge was in the landing and cruise configurations respectively. The higher modes results showed that the eccentric beam root stiffness did not have much influence on the skin natural frequency. When the beam stiffness was reduced the skin natural frequency only reduced by 4.1% for the landing case and 1.3% for the cruise configuration.
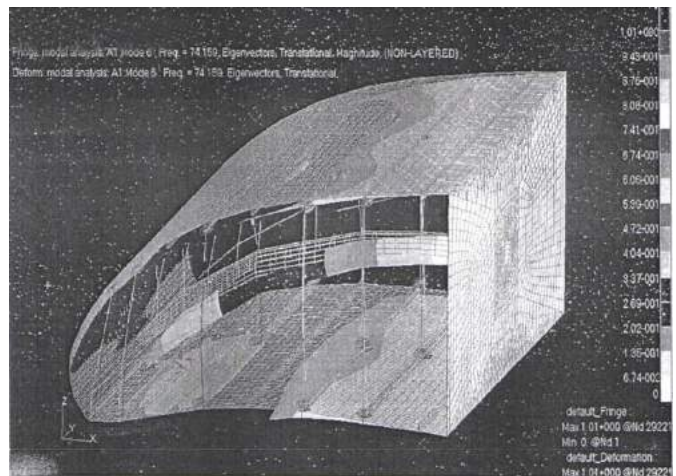
LEADING EDGE NATURAL FREQUENCIES IN LANDING CONFIGURATION

Mode number	Landing with leading edge fully deployed			
	100% stiffness		10% stiffness	
	Frequency(Hz)	Mode type	Frequency(Hz)	Mode type
1	20.559	Disc	20.478	Disc
2	38.086	Disc	37.523	Disc
3	54.607	Disc	53.468	Beam
4	67.898	Disc	54.608	Disc
5	77.372	Beam	54.609	Disc
6	77.372	Skin	74.159	Skin
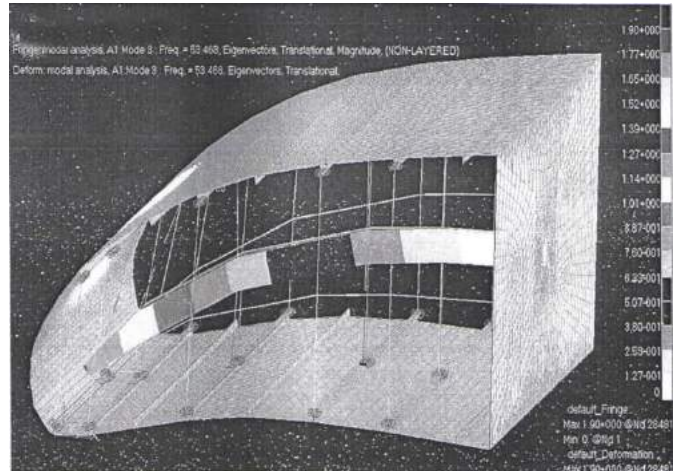
LEADING EDGE NATURAL FREQUENCIES IN CRUISE CONFIGURATION

Mode number	Landing with leading edge fully deployed			
	100% stiffness		10% stiffness	
	Frequency(Hz)	Mode type	Frequency(Hz)	Mode type
1	63.794	Beam	47.972	Beam
2	63.924	Disc	63.924	Disc
3	75.794	Skin	71.412	Skin
4	95.970	Disc	95.970	Disc
5	133.970	Skin	132.240	Skin
6	139.860	Skin	139.830	Skin

In landing configuration the first natural frequencies was lower than that in cruise, and the corresponding mode was a disc vibration mode. The first beam mode at landing condition occurred at 73Hz when the root stiffness was 100% and 53Hz when the root stiffness was 10%. Furthermore, the first beam vibration mode at cruise condition for the 100% beam root stiffness was 64Hz: however this was reduced by 25% when the beam root stiffness was reduced to 10%. The skin first vibration mode occurred instead at the higher modes: 77Hz and 134Hz when the leading edge was in the landing and cruise configurations respectively. The higher modes results showed that the eccentric beams root stiffness did not have much influence on the skin natural frequency. When the beam stiffness was reduced the skin natural frequency only reduced by 4.1% for the landing case and 1.3% for the cruise configuration. The following figures shows the leading edge first beam and skin vibration modes at landing with the eccentric beam stiffness reduced to 10%. Thus the figure shows the leading edge first beam and skin mode shapes at cruise with the eccentric beam stiffness reduced to 10%.
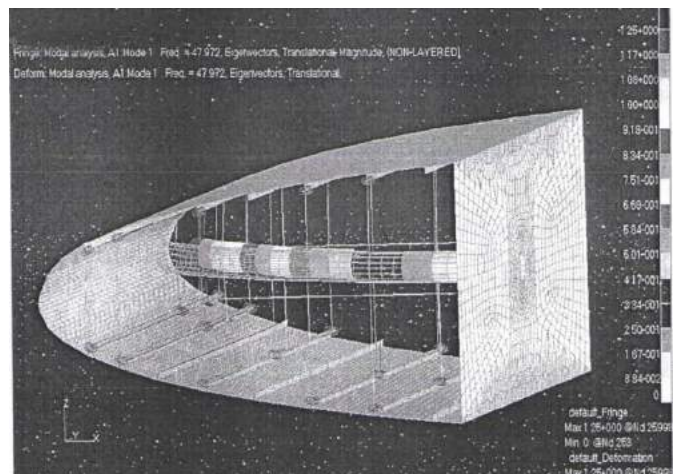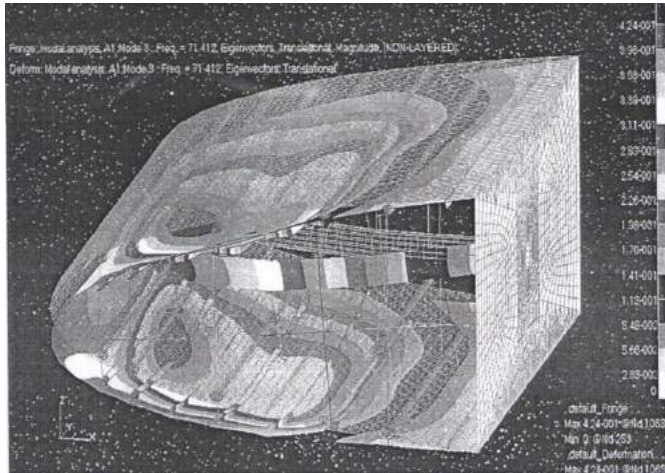
V. CONCLUSION

The design and analysis of the next generation wing concept started with the study of the composite wing box of the chosen reference wing. As the main configuration did not vary from a conventional box type structure the design process was kept at a preliminary stage, setting some key parameters which can be used for future studies. The attention instead, was focused on how this structure can be improved by increasing its strength and load carrying capability without adding significant weight penalty. The stress concentrations on spars and ribs webs, caused by the presence of cutouts, can be reduced by optimizing the cutout shape or by bonding reinforcement rings around the edge of the cutout. Significant stress reduction is achieved by using three reinforcement rings and their effectiveness depends on their stiffness. In particular, the use of carbon fiber tow placements enables to maximize the ratio of stress reduction and added structural weight. The reinforcement rings also have the capability of increasing the web buckling stability. In order to increase the strength of a composite joint in pulling the stiffness of the base panel must be maximized and good quality bonding must be used between the web and base panels in order to maximize the load transfer. For a composite joint in both pulling and shear it is of paramount importance to carefully choose the outer layers ply orientation. In particular by laying the outer layers fibers in the direction of the applied force it is possible to maximizes the load at which laminate matrix failure occurs.

REFERENCE

1. Arjyal, B.P., Katerelos, D.G., Galiotis, C. Measurement and modeling of stress concentration around a circular notch. Experimental Mechanics, 40(3), 2000, p.248-255.
2. Bailey, R., Wood, J. Stability characteristics of composite panels with various cutout geometries. Composite structures, 35(1), 1996,p. 21-31.
3. Bailey, R., Wood, J. Postbuckling behavior of square compression loaded graphite epoxy panels with square and elliptical cut-outs. Thin- walled structures, 28(3-4), 1997,p. 373-397.
4. Blake, J. I. R., Shenoi, R.A. House, J., Turton, T. Progressive damage analysis of tee joints with viscoelastic inserts. Composites Part A: Applied Science and Manufacturing, 32(5), 2001,p. 641-653.
5. De Boos, C., Guo, S., Zhou,L. The effect of core to skin thickness ratio and cutout reinforcements on composite sandwich panels. In: 15th International Conference on Composite/Nano Engineering (ICCE-15), Haikou, China, July 15-21 2007.
6. Eiblmeier, J., Loughlan, J. The influence of reinforcement ring width on the buckling response of carbon fiber composite panels with circular cut-outs. Composite Structures, 38(4), 1997, p. 609-622.
7. Engels, H., Becker, W. Optimization of hole reinforcements by doublers. Structural and Multidisciplinary Optimization, 20(1), 2000, p. 57-66.
8. Engels, H., Hansel, W., and Becker, W. Optimal design of hole reinforcements composite structures. Mechanics of composite materials, (5), 2002, p. 417-428.
9. Falzon, B. G., Steven, G. P., Xie, Y. M. Shape optimization of interior cut-outs in composite panels. Structural and Multidisciplinary Optimization, I I (1-2), 1996, P. 4349.
10. Guo, s. Stress concentration and buckling behavior of shear loaded composite panels with reinforced cutouts. Composite Structures, 80(1), 2007, p. 1-9.
11. Hyer, M. W., Lee, H. H. The use of curvilinear fiber format to improve buckling resistance of composite plates with central circular holes. Composite Structures, 18(3), 1991, p. 239-261.